A model to predict baffle effects in linear array of cMUTs

Audren Boulmé, Nicolas Sénégond, Franck Teston, Dominique Certon

ACOUSTICS 2012

A model to predict baffle effects in linear array of cMUTs

A. Boulmé, N. Sénégond, F. Teston and D. Certon

Université François-Rabelais de Tours, 10 Bd tonnellé, 37032 Tours, France
audren.boulme@univ-tours.fr

As for multi-source radiators, many studies have shown that the baffle effect phenomenon exists in cMUTs arrays too. This paper is a deep theoretical investigation of such phenomena which involve the apparition of cut-off frequencies in the radiated pressure. The linear array of cMUTs is modeled like a linear system. The input electrical quantities (voltage applied to each element of the array) are linked to the output acoustic quantities (pressure emitted by each element) with a global "transfer" matrix. The eigenvalues decomposition of the transfer matrix is used to discuss and to explain the origins of the baffle effect phenomenon.

1 Introduction

CMUTs are a very promising alternative to piezoelectricity in echographic imaging probes. Many authors have modeled cMUTs arrays but only few works have been dedicated to the simulation of devices working in real configuration, i.e. where each element is made of a finite number of cMUTs columns. The previous studies [1] and [2], pointed out that in such conditions, interactions between cMUTs could cause some strong cut-off frequencies in the useful frequency bandwidth, leading to undesirable oscillations at the end of the impulse response. This paper is a deep investigation of such interactions that we called after baffle effect.

Assuming that all the cMUTs cells have the same behavior in a column, a 2D matrix representation of the cMUTs array is developed. The cMUTs array is thus described as a linear system with multiple input/output ports that respectively correspond to each column of cMUTs in the array. Input/output ports are linked to each other through an acoustic admittance matrix that is sufficient to well-describe the behavior of a cMUTs array. We propose in this paper to use a modal analysis, i.e. eigenvectors decomposition, to understand origins of this baffle effect.

2 CMUTs array modeling

Multiple strategies can be used to simulate cMUTs array behavior. In this approach, each membrane is considered as a linear system and, in a same column, all the cells are assumed to be identical. cMUTs array modeling is performed in two steps. The first consists in calculating the response of one cMUT with 1D periodic boundary conditions, i.e. the response of one column of cMUTs. In the second step, the complete array is modeled by adding neighboring columns to the single column and by taking into account acoustic mutual interactions between each other.

2.1 Matrix modeling

As for the analysis presented in [3], cMUTs array can be modeled with a 2D matrix representation (Figure 1). This electroacoustic representation allows reducing the number of degrees of freedom to the number of columns.

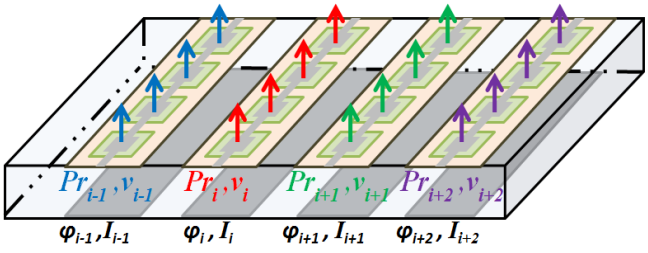

Figure 1: 2D representation of cMUTs array

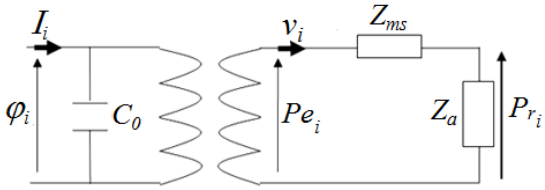

Figure 2: Equivalent electro-acoustic schema of one cMUT among a column of cMUTs

For the electrical part, the input/output quantities are the current I_i and the potential φ_i applied to each column of cMUTs and, for the acoustic part, variables are the mean radiated pressure Pr_i and the mean velocity displacement on the membrane surface v_i. The mechanical and electrostatic cross-talks with the substrate are not considered here. The first step of the model consists in considering one column of cMUTs only, without taking into account the others. Relationships between $[Pr_i, v_i]$ and $[I_i, \varphi_i]$ are established through an equivalent electro-acoustic model (Figure 2) computed with the same strategy presented in [4], where 1D periodic boundary conditions are applied to the cMUTs. Thus, for each column, it can be written:

$$Pr_i = Pe_i + (Z_a + Z_{ms})v_i \quad \text{with i=[1,...,N]} \tag{1}$$

Pe_i is the mean electrostatic pressure, Z_{ms} is the mechanical impedance of one membrane and Z_a is the self radiation impedance of one cMUT loaded with 1D periodic boundary conditions. N is the number of column per element.

To compute the electroacoustic response of the array, all columns have to be considered simultaneously and acoustic mutual interactions between each other must also be integrated in the model. For that, the radiation impedance of each column of cMUTs is decomposed as the sum of the self radiation impedance and all mutual radiation impedances Z^{ij}_{mut}. Z^{ij}_{mut} is the mutual radiation impedance between column i and column j. All impedances are grouped together in one matrix called the radiation matrix $[G]$. $[G]$ contains the self radiation impedance Z_a on the diagonal and out of the diagonal, the mutual impedance Z^{ij}_{mut}:

$$\left[G_{ij}\right] = \begin{cases} Z_a & ; \text{for i} = \text{j} \\ Z^{ij}_{mut} & ; \text{for i} \neq \text{j} \end{cases} \tag{2}$$

To determine the mutual impedance terms, it is assumed that the cMUTs vibrates like piston. In a similar way, a matrix global stiffness $[K_{ms}]$ can be constructed where the mechanical impedance terms appear. Here, it contains only the mechanical impedance Z_{ms} on the diagonal because cross-talks with the substrate are not considered.

$$\left[K_{ms}\right] = \begin{cases} Z_{ms} & ; \text{for i} = \text{j} \\ 0 & ; \text{for i} \neq \text{j} \end{cases} \tag{3}$$

The computation of the pressure emitted by one element of the array, made with N columns of cMUTs, leads to

solve a set of N linear equations where the input datum is the vector of the electrostatic pressures applied to each column [*Pe*], and the output one is the vector of average velocities of each columns [*v*]:

$$\begin{cases} \begin{bmatrix} v_1 \\ \dots \\ v_N \end{bmatrix} = \begin{bmatrix} Y_{11} & & Y_{1N} \\ & \dots & \\ Y_{N1} & & Y_{NN} \end{bmatrix} \begin{bmatrix} Pe_1 \\ \dots \\ Pe_N \end{bmatrix} ; \text{with} \\ [Y] = \left[[K_{ms}] + [G] \right]^{-1} \end{cases} \quad (4)$$

Electro-acoustic properties of one element of the array are totally described by its admittance matrix [*Y*]. The electrical admittance Y_{array} of one element is deduced from [*Y*]. It is easily to obtain its expression after simple manipulations:

$$Y_{array} = jC_p\omega + jNN_{cmut}C_0\omega + N_{cmut}\phi^2 \sum_{j=1}^{N}\sum_{i=1}^{N} Y_{ij} \quad (5)$$

N_{cmut} is the number of cMUTs per column, C_0 is the static capacitance of one cMUT, C_p is the parasitic capacitance of the cMUTs array, and ϕ is the transformer ratio.

2.2 Experimental confrontation

In order to validate the model, the simulated and the experimental response of one element are compared. The studied element is composed of 4 columns and 57 lines of square-shaped cells. Each cell are made with a silicon nitride membrane of 25x25µm² partially covered (50% arena) with an aluminum electrode. Cavities were sealed under vacuum; so there is no squeeze film effect. The thickness and the properties of each layer are listed in Table 1. The pitches are 15µm between two columns and 11µm between two lines.

Table 1: Dimensions of cMUTs membranes and physical properties of material used for simulation

Layer	Gap (Vacuum)	Membrane (SiN)	Electrode (Al)
Thickness (nm)	200	450	350
Width (µm)	n/a	25	18
Young's modulus (GPa)	n/a	220	68
Poisson ratio	n/a	0.25	0.35
Density (kg.m-3)	n/a	3300	2700
Relative permittivity	n/a	7.5	

First, the element has been characterized following the method based on electrical impedance measurement in air, presented in [6]. The measured fundamental resonance frequency, the collapse voltage, and the parasitic capacitance are respectively 10.8 MHz, 60 V, and 4.8 pF. The set of electrical impedance curves for different bias voltages was used to fit input data of the model. The electrical reactance obtained for a bias voltage of 30V and the electromechanical coupling factor are compared to the model in Figure 3. Despite a good agreement until 50V, a strong deviation is observed around the collapse voltage. This discrepancy is due to the inhomogeneity between cells.

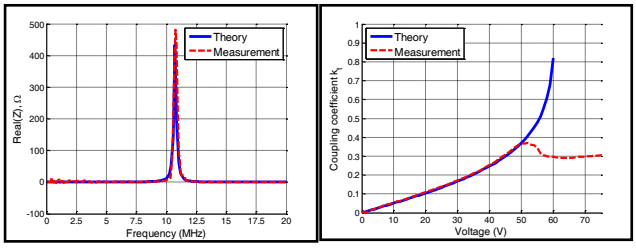

Figure 3: Theoretical and experimental real part of the electrical impedance for a bias voltage of 30V (left part) and theoretical and experimental coupling coefficient (right part)

With the set of parameters determined from measurements in air, the theoretical impedance of cMUTs loaded by oil was computed and compared to the experimental data (Figure 4). A good agreement is observed. But the main feature on this result is the 3.8 MHz cut-off frequency which corresponds to the previously discussed baffle effect.

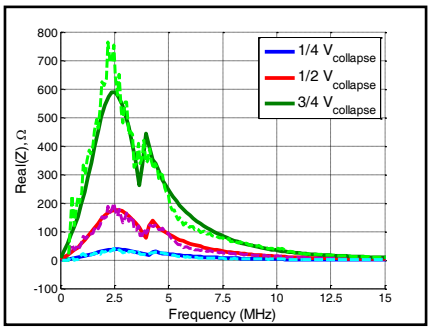

Figure 4: Theoretical (continuous curves) and experimental (dashed curves) real part of the electrical impedance for three bias voltages

3 Modal decomposition of the pressure field

The approach presented here is an original investigation of the baffle effect based on the normal mode theory.

3.1 Modal decomposition of the admittance matrix

The origin of baffle effect can be explained with properties of the acoustic admittance matrix [*Y*]. The objective of this study consists in identifying the normal radiation mode of the cMUTs array, by mean of the eigenvalue decomposition of the matrix [*Y*]. Since [*Y*] is a square matrix, thanks to the matrix theory [7], we can rewrite [*Y*] under the form:

$$[Y] = [V^e][\lambda][V^e]^{-1} \quad (6)$$

Where [λ] is the diagonal matrix of the eigenvalues of [*Y*] and [V^e] is the orthonormal matrix composed by the corresponding eigenvectors (arranged in columns).

The equation (4) becomes:

$$[v] = [V^e][\lambda][V^e]^{-1}[Pe] \quad (7)$$

[α] are the projection coefficients of the electrostatic pressure vector onto the eigenvectors base:

$$[\alpha]=\left[V^e\right]^{-1}[Pe] \tag{8}$$

So equation (7) becomes:

$$[v]=\sum_{i=1}^{N}\alpha_i\,\lambda_i\left[V^e\right]_i \tag{9}$$

Thus, the mean velocity of each column, $[v]$, is clearly identified as a linear combination of all the normal radiation modes of the cMUTs array.

Since the stiffness matrix $[K_{ms}]$ is diagonal, the eigenvectors of the matrix $[Y]$ and those of the matrix $[G]$ are identical and independent of the membrane mechanical impedance. More, the eigenvalues of admittance λ_i can be redefined using some classical properties [7] of the square matrix as:

$$\lambda_i=\frac{1}{\gamma_i+Z_{ms}} \tag{10}$$

γ_i are the eigenvalues of the acoustic radiation matrix $[G]$. This relation expresses, for each mode, the physical coupling between membrane elasticity and the mass of fluid.

3.2 Illustrative example

In this subsection, the modal decomposition of the transfer matrix $[Y]$ is applied for the experimental case previously described in the section 2.2. Since each element is composed of 4 columns, $[Y]$ has 4 eigenvectors and 4 eigenvalues. Each normal mode is a specific combination of four elementary radiating acoustic line sources. The first mode is the case where the four columns are vibrating in phase, it will be noted (++++). The second is an asymmetric one and is a combination of two lines vibrating in phase while the two others are in opposition: (++--). The third is symmetric, the two outer lines are in phase while the centers lines are in opposition: (+--+). Finally the last one is (+-+-). Moreover, all components of the electrostatic pressure vector $[P_e]$ are fixed to 1 then, only symmetrical modes are excited. Consequently, the pressure radiated by one element composed of 4 columns of cMUTs is a linear combination of the mode 1 and the mode 3.

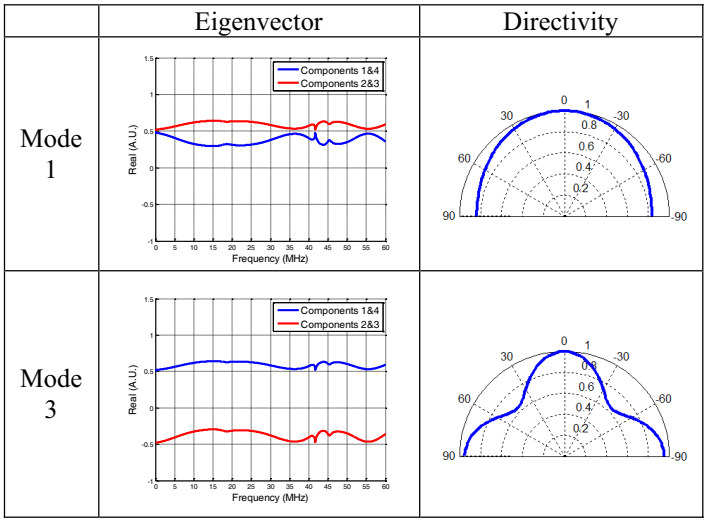

Figure 5: Eigenvectors and directivities for the modes 1 and 3

In Figure 5, the eigenvectors components are represented versus the frequency for the mode 1 and the mode 3. The main features of theses curves are the apparition of cut-off frequencies. The first, for $f_{cx}=c/d_x \approx$ 37.5MHz, corresponds to the case where the acoustic wavelength is equal to the horizontal periodic pitch d_x. The second for $f_{cy}=c/d_y \approx$ 41.7MHz is the case where one acoustic wavelength separates two cMUTs along the elevation. This second frequency corresponds to the radiation of the second spatial harmonic of the 1D periodic array of cMUTs. Under this limit, each column of cMUTs radiates like a line source.

The directivity pattern of mode 1 and mode 3 at 5 MHz, is showed on the right of the Figure 5. As expected, the main radiation axis of the mode 1 is perpendicular to the plane of the transducer while the mode 3 radiates a part of its energy in the plane of the transducer.

As it was previously demonstrated with the equation (10), eigenvalues allow observing the membrane mechanical impact in addition with cMUTs layout. For the two modes, minima are clearly observed at f_m=26.7MHz and f_{cy}=41.7MHz (Figure 6). The first minimum is a cut-off frequency caused by the second resonance mode of membranes (this mode is anti-symmetric and not electrically coupled). The second minimum is due to the periodicity along the elevation From the analyses of the mode 3, a maximum is clearly observable at f=3.8MHz. Such "local resonance" of mode 3 is the baffle effect and produces cut-offs observed in the response of the array (see Figure 4).The maximum can be interpreted as a local mass-spring resonance where the energy is trapped at the surface of the transducer. The evolution of the mode 1 is more classical since the well-known large bandwidth response of cMUTs transducer can be identified. This mode defines the central frequency and the bandwidth of the transducer. It is interesting to note that mode 1 is mainly dominant except when mode 3 is locally resonating.

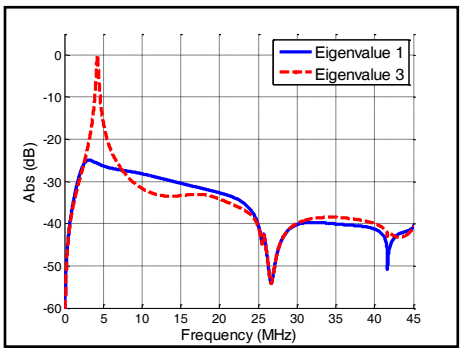

Figure 6: Eigenvalues versus frequency for modes 1 and 3

All the properties of mode 1 and mode 3 will impact the shape of the pressure spectrum (Figure 7). The central frequency and bandwidth are those defined by the mode 1. At the resonance frequency of the mode 3, local disturbances appear in the pressure spectrum and in the directivity pattern too (Figure 8). The cut-off frequency is strongest around an angle of ninety degrees. This phenomenon is explained by the fact that the mode 3 radiates energy in the plane of the transducer.

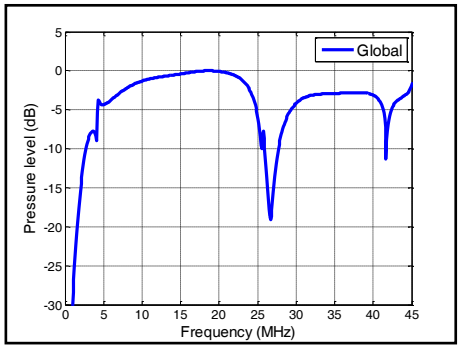

Figure 7: Pressure radiated by the cMUTs array element. This simulation is achieved in water at 60mm.The pressure level reference is 155Pa/V.

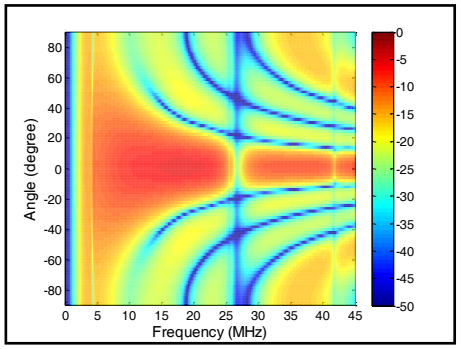

Figure 8: Diffraction field pattern of the cMUTs array element. This simulation is achieved in water at 60mm.The pressure level reference is 155Pa/V.

4 Parametric study

In this section, a parametric study is conducted in order to explore separately the impact of the mechanical impedance, the pitch between columns, and the number of columns. The cMUTs device is the same than the one presented in section 2.2.

4.1 Influence of the mechanical impedance

In order to change the mechanical impedance, two membranes parameters can be modified: the thickness or the size. We have done the choice to change only the thickness without modifying the layout. The pressure field spectrum at 60 mm from the transducer is reported in Figure 9 for mode 1 and in Figure 10 for the mode 3. For all simulations, since the layout was not changed, the cut-off frequency due to periodicity stays at about 41.7 MHz. On the mode 1, the increase of the mechanical impedance shifts the central frequency and the bandwidth toward a higher frequency. The impact of the mechanical impedance on the local resonance of the mode 3 is smaller: a slow shift is also observable. So, the impact of the baffle effect on the cMUTs response is reduced when the mechanical impedance is increased, since it appears in the low frequency domain of the transducer bandwidth. This is probably the reason for which the baffle effect was poorly discussed up today. In the literature, the majority of experimental devices are made with a large thickness membrane, typically 1µm. An optimal value for the thickness is pointed out for the mode 1: 550 nm. With 550 nm, the shape of the frequency response is the flattest.

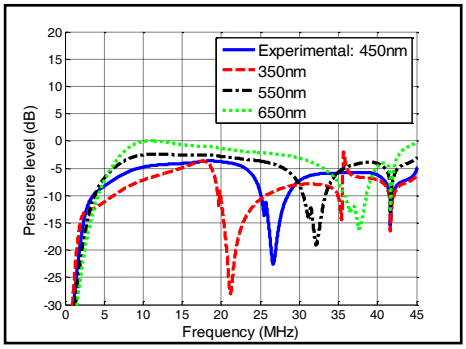

Figure 9: Variation of the pressure radiated by the mode 1 for various membranes thickness. This simulation is achieved in water at 60mm.The pressure level reference is 216Pa/V.

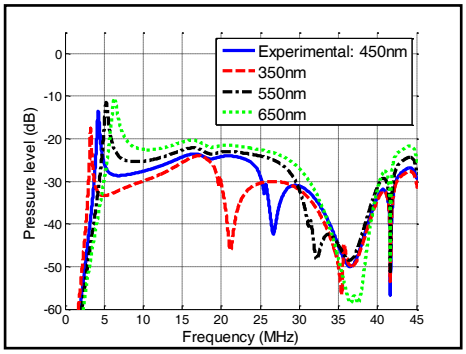

Figure 10: Variation of the pressure radiated by the mode 3 for various membranes thickness. This simulation is achieved in water at 60mm.The pressure level reference is 216Pa/V.

4.2 Influence of the pitch between two columns

In this subsection, the mechanical impedance is fixed and only the horizontal pitch varied (Figure 11 and Figure 12). As for the mechanical impedance, an optimal configuration in terms of sensitivity and bandwidth is found between 15µm and 25µm. This result is interesting because, contrary to the literature information, the best configuration is not obtained for the smallest pitch. Moreover, the increase of the pitch reduces the amplitude of the local resonance of the mode 3 (Figure 12), and consequently the baffle effect. The case where the pitch is the largest is an extreme situation where the cut-off frequency due to the horizontal periodicity arises at a lower frequency than the second resonance mode of the membrane. The cut-off frequency caused by the periodicity along the elevation is unchanged (41.7 MHz).

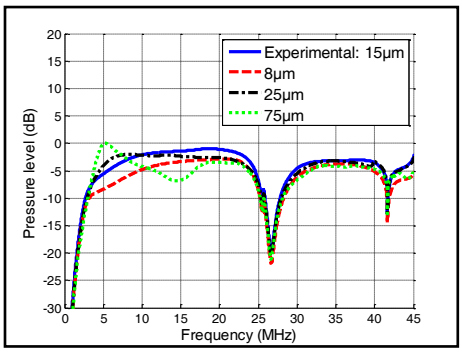

Figure 11: Variation of the pressure radiated by the mode 1 for various inter-columns pitches. This simulation is achieved in water at 60mm.The pressure level reference is 158Pa/V.

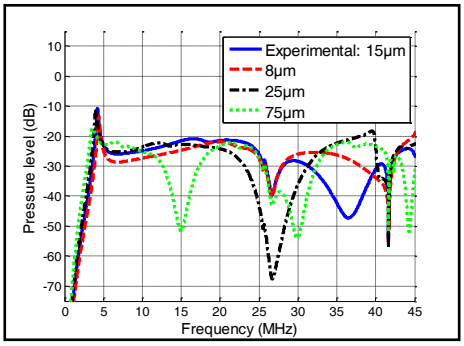

Figure 12: Variation of the pressure radiated by the mode 3 for various inter-columns pitches. This simulation is achieved in water at 60mm.The pressure level reference is 158Pa/V.

4.3 Influence of the number of column

The last parameter is the number of column per element. Four cases are compared in Figure 13 : 4, 6, 8 and 10 columns. The more the number increases, the more the baffle effect reduces. The modal analysis can help to interpret this result. Indeed, when the number of column increases, the number of normal modes increases too. However, in the far field, the summation of such parasitic modes is not constructive and consequently leads to a real reduction of the baffle effect on the acoustic performance of the transducer. Practically, this property shows that when the number of column per element is small (typically lower than 6), it is better to use synthetic beamforming techniques for which acoustic emission is realized with a group of several emitters (which arbitrarily increases the number of column) instead of the "Delay and Sum" method for which the elements are driven separately.

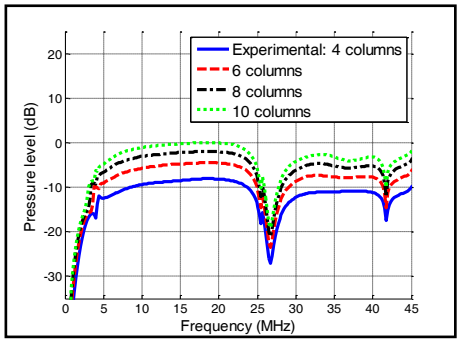

Figure 13: Variation of the pressure radiated by the cMUTs element for various numbers of column. This simulation is achieved in water at 60mm.The pressure level reference is 392 Pa/V.

5 Conclusion

A linear model, based on a matrix formalism, has been developed in order to predict the electroacoustic response of cMUTs array and particularly the central frequency and the bandwidth. A global transfer matrix is computed from which the pressure field radiated by one element is expressed as a linear combination of voltages on each cMUT. The normal mode theory applied to the transfer matrix of the array provides an interesting interpretation of the baffle effect in such devices. Among all eigenmodes of the matrix, one mode corresponds to the case where all columns of cMUTs vibrate in phase, this is the useful mode for acoustic imaging. The other modes are another combination of multi-polar sources for which all cMUTs do not vibrate in phase. Such modes are parasitic and cause the baffle effect. More precisely, it has been shown that, for each "parasitic" mode, it existed one particular frequency for which the membrane oscillated. At this resonance, there is a strong coupling between the membrane elasticity and the fluid mass. Then, it produces a local trapping of the acoustic energy and small oscillations in the response of the array. Note that some authors proposed to use such "local trapping modes" for sensing applications, for example the measurement of fluid acoustic properties. In addition, an impact on the directivity pattern has also been predicted with a reduction of the beam-width in the vicinity of the cut-off frequencies. Finally, some interesting trade-offs has been identified since it has been shown that the pitch and the membrane thickness can be simultaneously tuned in order to reject or diminish baffle effects.

Acknowledgments

The Agence National de la Recherche and the Fonds Européen de développement Régional are acknowledged for their financial support (COSTUM ANR-09-TECS-005-01 and FEDER COSTUM II 2657-33868).

References

[1] S. Ballandras, M. Wilm, and W. Daniau, "Periodic finite element/boundary element modeling of capacitive micromachined ultrasonic transducer," *Journal of Applied Physics*, vol. 97, p. 1, 2005.

[2] A. Caronti, A. Savoia, G. Caliano, and M. Pappalardo, "Acoustic coupling in capacitive microfabricated ultrasonic transducers: modeling and experiments," *IEEE-UFFC*, vol. 52, no. 12, pp. 2220-2234, 2005.

[3] D. Certon, F. Patat, C. Meynier, and F. Teston, "Collective Behavior of cMUT Cells for the Prediction of Electroacoustic Response and Directivity Pattern," *in proceedings of UFFC*, pp. 1967-1970, 2006.

[4] D. Certon, F. Teston, and F. Patat, "A finite difference model For cMUT devices," *IEEE-UFFC*, vol. 52, no. 12, pp. 2199-2210, 2005.

[5] C. Meynier, F. Teston, and D. Certon, "A multiscale model for array of capacitive micromachined ultrasonic transducers," *Journal of the Acoustical Society of America*, vol. 128, 2010.

[6] F. Teston, C. Meynier, E. Jeanne, N. Felix, and D. Certon, "Characterization Standard of CMUT Devices Based on Electrical Impedance Measurements," *in proceedings of UFFC*, pp. 1963-1966, 2006.

[7] J. H. Wilkinson, *The algebraic eigenvalue problems*, Clarendon Press, Oxford University Press, 1965.